is too tightly wedged in the heme crevice to undergo the migration reaction in the absence of some degree of protein denaturation. Alternatively, the oxidation potential of the myoglobin complex may be such that it is not readily accessible to exogenous oxidizing agents.

Recent work with several rat liver cytochrome P450 isozymes has shown that they form iron-phenyl complexes and, more importantly, that potassium ferricyanide promotes the iron-nitrogen shift within the undenatured protein complexes to give only two of the four possible *N*-phenyl adducts.[16] The isomer separation and identification reported here provide the key to the use of this N-arylation regiospecificity to define the topologies of the active sites of membrane-bound cytochrome P450 enzymes and possibly other hemoproteins with open (substrate-accessible) heme binding sites.

Acknowledgment. This work was supported by Grants DK30297, GM 32488, and GM 25515 from the National Institutes of Health. Mass spectra were kindly obtained by Dr. David Maltby in the Biomedical, Bioorganic Mass Spectrometry Facility of the University of California, San Francisco (A. Burlingame, Director), supported by National Institutes of Health Grants RR 01614 and P-30 DK 26743.

Registry No. Isomer 1, 136006-23-0; isomer 2, 136006-24-1; isomer 3, 136006-25-2; isomer 4, 136006-26-3; heme, 14875-96-8; phenylhydrazine, 100-63-0.

Photochemistry of Intercalated Quaternary Diazaaromatic Salts

Anne M. Brun and Anthony Harriman*

Contribution from the Center for Fast Kinetics Research, The University of Texas at Austin, Austin, Texas 78712. *Received April 18, 1991*

Abstract: Certain quaternary diazaaromatic salts intercalate between base pairs in calf thymus DNA and in synthetic polynucleotides. The intense fluorescence of these salts, as observed in dilute aqueous solution, is quenched upon intercalation due to electron abstraction from an adjacent base. This reaction is not sequence-specific. The resultant radical cation of the quaternary salt decays within 100 ps. Individual nucleotide monophosphates also transfer an electron to the excited singlet state of the salts, both in fluid solution and after complexation in the ground state. Illumination of a salt/nucleotide ground-state complex generates the corresponding radical ion pair, which decays within 100 ns. These results indicate that photoinduced electron-transfer processes involving intercalated dye molecules occur on faster (i.e., 2500-fold) time scales than for the corresponding complexed reactants and are highly reversible.

Flat, cationic molecules can interact strongly with polynucleotides and, provided the cation is of the appropriate dimensions, intercalate into the DNA strand.[1] Many such cations have been reported, including metalloporphyrins,[2-4] ethidium bromide,[5] methylene blue,[6] and heterocycles,[7-10] and several have been shown to induce strand scission upon light or electrical stimulation. Of particular interest is the observation that certain diazapyrenium dications associate with polynucleotides and cause their photocleavage under anaerobic irradiation with visible light.[11-13] These compounds show intense fluorescence in solution that is quenched upon binding to certain polynucleotides.[11-13] In view of the fact that such quaternary salts are easily reduced,[14] it can be speculated that fluorescence quenching is due to electron abstraction from a nucleic acid base or ribose by the singlet excited state of the dye.[13,15] We have studied the photochemistry of this system using laser flash photolysis techniques and found that quaternary diazaaromatic dyes are able to abstract an electron from nucleotides and polynucleotides, under illumination with visible light, but the process is reversible.

Experimental Section

N,N'-Dimethyl-2,7-diazapyrene bis(tetrafluoroborate) (DAP^{2+}) and *N,N'*-dimethylanthra[2,1,9-*def*:6,5,10-*d'e'f'*]diisoquinoline dichloride

(1) Saenger, W. *Principles of Nucleic Acid Structure*; Springer-Verlag: New York, 1984.
(2) Fiel, R. J.; Munson, B. R. *Nucleic Acids Res.* **1980**, *8*, 2935.
(3) (a) Pasternack, R. F.; Gibbs, E. J.; Villafranca, J. J. *Biochemistry* **1983**, *22*, 2406, 5409. (b) Kelly, J. M.; Murphy, M. J. *Nucleic Acids Res.* **1985**, *13*, 167. (c) Geacintov, N. E.; Ibanez, V.; Rougee, M.; Bensasson, R. V. *Biochemistry* **1987**, *26*, 3087.
(4) Hamilton, A. D.; Lehn, J.-M.; Sessler, J. L. *J. Am. Chem. Soc.* **1988**, *108*, 5158.
(5) (a) Le Pecq, J. B.; Yot, P.; Paoletti, C. *C. R. Seances Acad. Sci., Ser. D* **1964**, *259*, 1786. (b) Waring, M. J. *J. Mol. Biol.* **1965**, *13*, 269. (c) Le Pecq, J. B.; Paoletti, C. *J. Mol. Biol.* **1967**, *27*, 87. (d) Burns, V. W. F. *Arch. Biochem. Biophys.* **1969**, *183*, 420. (e) Olmsted, J. O., III; Kearns, D. R. *Biochemistry* **1977**, *16*, 3647. (f) Fromherz, P.; Rieger, B. *J. Am. Chem. Soc.* **1986**, *108*, 5361.
(6) (a) Mueller, W.; Crothers, D. M. *Eur. J. Biochem.* **1975**, *54*, 267. (b) Friedman, Th.; Brown, D. M. *Nucleic Acids Res.* **1978**, *5*, 615. (c) Kittler, L.; Lober, G.; Gollnick, F. A.; Berg, H. *J. Electroanal. Chem.* **1980**, *116*, 503. (d) Kelly, J. M.; van der Putten, W. J. M.; McConnell, D. J. *Photochem. Photobiol.* **1087**, *45*, 167.
(7) Berman, H. M.; Young, P. R. *Annu. Rev. Biophys. Bioeng.* **1981**, *10*, 87. (b) Dougherty, G.; Pilbrow, J. R. *Int. J. Biochem.* **1984**, *16*, 1179. (c) Zimmerman, H. W. *Angew. Chem.* **1986**, *25*, 115.
(8) (a) Bowler, B. E.; Hollis, L. S.; Lippard, S. J. *J. Am. Chem. Soc.* **1984**, *106*, 6102. (b) Freifelder, D.; Davison, P. F.; Geiduschek, E. P. *Biophys. J.* **1961**, *1*, 289.
(9) (a) Berg, H. *Bioelectrochem. Bioenerg.* **1978**, *5*, 347. (b) Kittler, L.; Lober, G.; Gollmick, F. A.; Berg, H. *Bioelectrochem. Bioenerg.* **1980**, *7*, 503.
(10) Jazwinski, J.; Blacker, A. J.; Lehn, J.-M.; Cesario, M.; Guilhem, J.; Pascard, C. *Tetrahedron Lett.* **1987**, 6057.
(11) Blacker, A. J.; Jazwinski, J.; Lehn, J.-M. *Helv. Chim. Acta* **1987**, *70*, 1.
(12) (a) Lehn, J.-M. In *Supramolecular Photochemistry*; Balzani, V., Ed.; NATO ASI Series C; Reidel, Dordrecht, 1987; Vol. 214, p 29. (b) Blacker, A. J.; Jazwinski, J.; Lehn, J.-M.; Wilhelm, F. X. *J. Chem. Soc., Chem. Commun.* **1986**, 1035.
(13) (a) Slama-Schwok, A.; Jazwinski, J.; Bere, A.; Montenay-Garestier, T.; Rougée, M.; Hélène, C.; Lehn, J.-M. *Biochemistry* **1989**, *28*, 3227. (b) Slama-Schwok, A.; Rougée, M.; Ibanez, V.; Geacintov, N. E.; Montenay-Garestier, T.; Lehn, J.-M.; Hélène, C. *Biochemistry* **1989**, *28*, 3234.
(14) Hünig, S.; Grosse, J. *Tetrahedron Lett.* **1968**, 2599; **1968**, 4139.
(15) Beddard, G. S.; Kelly, J. M.; van der Putten, W. J. M. *J. Chem. Soc., Chem. Commun.* **1990**, 1346.

0002-7863/91/1513-8153$02.50/0

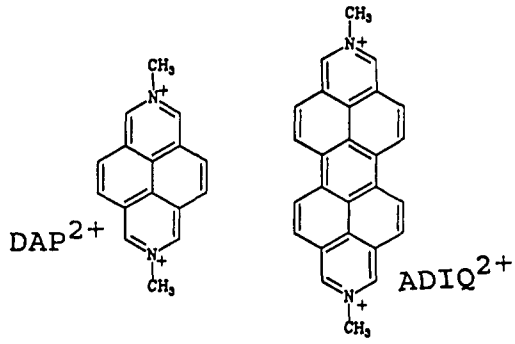

Figure 1. Structures for the quaternary diazaaromatic compounds.

($ADIQ^{2+}$) were prepared and purified according to the method of Hünig et al.;[16] structures are shown in Figure 1. Both compounds gave satisfactory ^1H NMR (in D_2O), MS, and elemental analyses. Highly polymerized deoxyribonucleic acid, sodium salt (DNA), from calf thymus, was purchased from Sigma Chemical Co. and used as received. Stock solutions of DNA were prepared by dissolution overnight in 5 mM phosphate pH 7 buffer and were stored at 4 °C in the dark for short periods only. Concentrations of DNA per nucleotide phosphate were determined by absorption spectroscopy using a molar extinction coefficient (ϵ) of 6600 M^{-1} cm^{-1} at 260 nm.[17] Samples of 2'-deoxyadenosine-5'-monophosphate, sodium salt (dAMP), 2'-deoxycytidine-5'-monophosphate, sodium salt (dCMP), and 2'-deoxyguanosine-5'-monophosphate, sodium salt (dGMP), were purchased from Sigma and stored at 0 °C. Samples of double-stranded copolymer consisting of alternating deoxyadenylic acid and deoxythymidylic acid, sodium salt (poly[dA-dT]) (ϵ_{260} = 6600 M^{-1} cm^{-1})[18] and of a random copolymer comprising deoxyguanylic acid and deoxycytidylic acid, sodium salt (poly[dG-dC]) (ϵ_{260} = 8400 M^{-1} cm^{-1})[18] were obtained from Sigma and stored at 0 °C. Water was distilled fresh from a Millipore-Q system.

Absorption spectra were recorded with a Hitachi U3210 spectrophotometer, and fluorescence spectra were recorded with a Perkin-Elmer LS5 spectrofluorimeter, after correction for spectral responses of the instrument.[19] Fluorescence quantum yields were calculated by using the optically dilute method with quinine bisulphate in 1 N H_2SO_4 as reference,[20] for which the fluorescence quantum yield was taken to be 0.55. Both DAP^{2+} and $ADIQ^{2+}$ exhibit concentration-dependent fluorescence yields,[13] and quantitative studies demand the use of very low concentrations of fluorophore. Excited-singlet-state lifetimes were determined by the time-correlated, single-photon-counting technique[21] using a mode-locked Nd-YAG synchronously pumped, cavity-dumped Rhodamine 6G dye laser. The excitation wavelength was 300 nm, and fluorescence was separated from scattered laser light by glass cutoff filters. Data analysis was made after deconvolution of the instrument response function (fwhm = 50 ps). Titrations were carried out by adding successive amounts of aqueous solutions of either DAP^{2+} or $ADIQ^{2+}$ to a freshly prepared DNA stock solution. All solutions were air-equilibrated.

Laser flash photolysis studies were made with a frequency-tripled Nd-YAG laser. For nanosecond time scale studies, the laser was Q-switched and a pulsed Xe arc lamp was used as the monitoring beam. The laser intensity was attenuated with metal screen filters and calibrated with respect to pyrene in cyclohexane.[22] Solutions were purged thoroughly with N_2 before and during the experiment. Spectra were recorded point-by-point, with five individual records being computer-averaged at each wavelength. Kinetic studies were made at fixed wavelengths, with 50 individual records being averaged, base line corrected, and analyzed by computer nonlinear, least-squares iterative procedures. Improved time resolution was obtained with a mode-locked laser operated in the pump-probe technique.[23] Approximately 300 individual shots were averaged at each time delay, base line corrected, and analyzed by computer iterations.

Singlet molecular oxygen was detected by time-resolved luminescence spectroscopy at 1270 nm.[24] Solutions of quaternary salt in D_2O were adjusted to possess an absorbance at 355 nm of ca. 0.2 and were saturated with O_2. Laser intensities were attenuated over a wide range by using neutral density filters, and the yield of singlet oxygen was derived by computer extrapolation of the first-order decay profile to the center of the laser pulse. For each record, 50 individual laser pulses were averaged. The detector was calibrated by using zinc tetrakis(*N*-methyl-4-pyridyl)porphyrin in D_2O.[25]

Pulse radiolysis experiments were performredd with the CFKR 4-MeV Van de Graaff electron beam accelerator, which delivers 10-ns pulses of electrons. The solutions contained DAP^{2+} (2×10^{-4} M) in N_2-purged aqueous solution with phosphate buffer (1 mM, pH 7) and 2-propanol (0.4 M). Under such conditions, the quaternary salt is reduced by hydrated electrons and 2-hydroxypropyl radicals with a radiation yield of $G = 0.6$. One-electron reduction of $ADIQ^{2+}$ was accomplished at lower concentration (3×10^{-5} M), to avoid association of reactants and/or products, in the presence of 2-butanol (0.4 M); the expected radiation yield is $G = 0.27$. Absorption spectra for the resultant one-electron reduction products were recorded point-by-point, and dosimetry was made with methylviologen in N_2-saturated aqueous solution (ϵ at 605 nm is 13 700 M^{-1} cm^{-1}).[26] Similar studies were made with the quaternary salt intercalated into DNA (P/D = 20).

Cyclic voltammetry studies were made with a Pine Instruments Model AFRDE4 potentiostat and a conventional three-electrode setup. Solutions contained the quaternary salt (1×10^{-4} M), KCl (0.2 M), and phosphate buffer (1 mM, pH 7) and were purged thoroughly with N_2. The working electrode was a highly polished glassy-carbon microdisk that was used in conjunction with a Pt wire counter electrode and an SCE reference. Similar voltammograms were recorded with the quaternary salt bound to DNA at various molar ratios.

Table I. Photophysical and Redox Properties Derived for DAP^{2+} and $ADIQ^{2+}$ in Neutral Aqueous Solution

property	DAP^{2+}	$ADIQ^{2+}$
Φ_f[a]	0.63	0.79
τ_s (ns)[b]	9.0	24.4
Φ_t[c]	0.17	0.12
τ_t (ms)[d]	0.8	1.0
k_{rad} (10^7 s^{-1})	6.2	4.1
Φ_Δ[c]	0.14	0.08
E_p^1 (V vs NHE)[e]	−0.26	−0.34
E_p^2 (V vs NHE)[e]	−0.42	−0.47
$1/K_{dis}$ (M)[f]	510	160

[a] ±5%. [b] ±1 ns. [c] ±15%. [d] ±0.1 ms. [e] ±20 mV. [f] ±20%.

Results and Discussion

Photophysical and Redox Properties of the Quaternary Salts. Absorption and fluorescence spectra for DAP^{2+} and $ADIQ^{2+}$ have been reported previously.[11,13,16] Both compounds fluoresce strongly, quantum yields (Φ_f) measured in aerated aqueous solution are given in Table I, and the fluorescence excitation spectra show good agreement with the corresponding absorption spectra. Fluorescence lifetimes (τ_s) are comparatively long (Table I), and the radiative rate constants (k_{rad}), calculated from the Strickler–Berg equation,[27] remain in good agreement with the experimental ($k_{rad} = \Phi_f/\tau_s$) values.

The triplet excited states of these compounds in N_2-saturated, neutral aqueous solution can be observed readily after excitation with a 10-ns laser pulse at 355 nm. The triplet differential absorption spectrum recorded for DAP^{2+} (Figure 2a) shows a maximum at 410 nm and retains features similar to those characteristic of pyrene in organic solvents.[22] The corresponding spectrum recorded for $ADIQ^{2+}$ is shown in Figure 2b. Both triplets decay by first-order kinetics at low laser intensity, the derived lifetimes (τ_t) are collected in Table I, but triplet–triplet annihilation becomes important at higher intensity. The triplets react quantitatively with molecular oxygen, producing singlet oxygen $O_2(^1\Delta_g)$ as detected[24] by time-resolved luminescence spectroscopy in D_2O,

(16) Hünig, S.; Gross, J.; Lier, E. F.; Quast, H. *Liebigs Ann. Chem.* **1973**, 339.
(17) Reichmann, M. E.; Rice, S. A.; Thomas, C. A.; Doty, P. *J. Am. Chem. Soc.* **1954**, *76*, 3047.
(18) Kelly, J. M.; van der Putten, W. J. M.; McConnell, D. J. *Photochem. Photobiol.* **1987**, *45*, 167.
(19) Argauer, R. J.; White, C. E. *Anal. Chem.* **1964**, *36*, 368.
(20) (a) Meilhuish, W. H. *J. Phys. Chem.* **1961**, *65*, 229. (b) Meech, S. R.; Phillips, D. *J. Photochem.* **1983**, *23*, 193.
(21) O'Connor, D. V.; Phillips, D. *Time Correlated Single Photon Counting*; Academic Press: London, 1984.
(22) Carmichael, I.; Hug, G. L. *J. Phys. Chem. Ref. Data* **1986**, *15*, 1.
(23) Atherton, S. J.; Hubig, S. M.; Callen, T. J.; Duncanson, J. A.; Snowden, P. T.; Rodgers, M. A. J. *J. Phys. Chem.* **1987**, *91*, 3137.
(24) Rodgers, M. A. J.; Snowden, P. T. *J. Am. Chem. Soc.* **1982**, *104*, 5341.
(25) Verlhac, J. K.; Gaudemar, A.; Kraljic, I. *Nouv. J. Chim.* **1984**, *8*, 401.
(26) Watanabe, T.; Honda, K. *J. Phys. Chem.* **1982**, *86*, 2617.
(27) Strickler, S. J.; Berg, D. J. *J. Chem. Phys.* **1962**, *37*, 814.

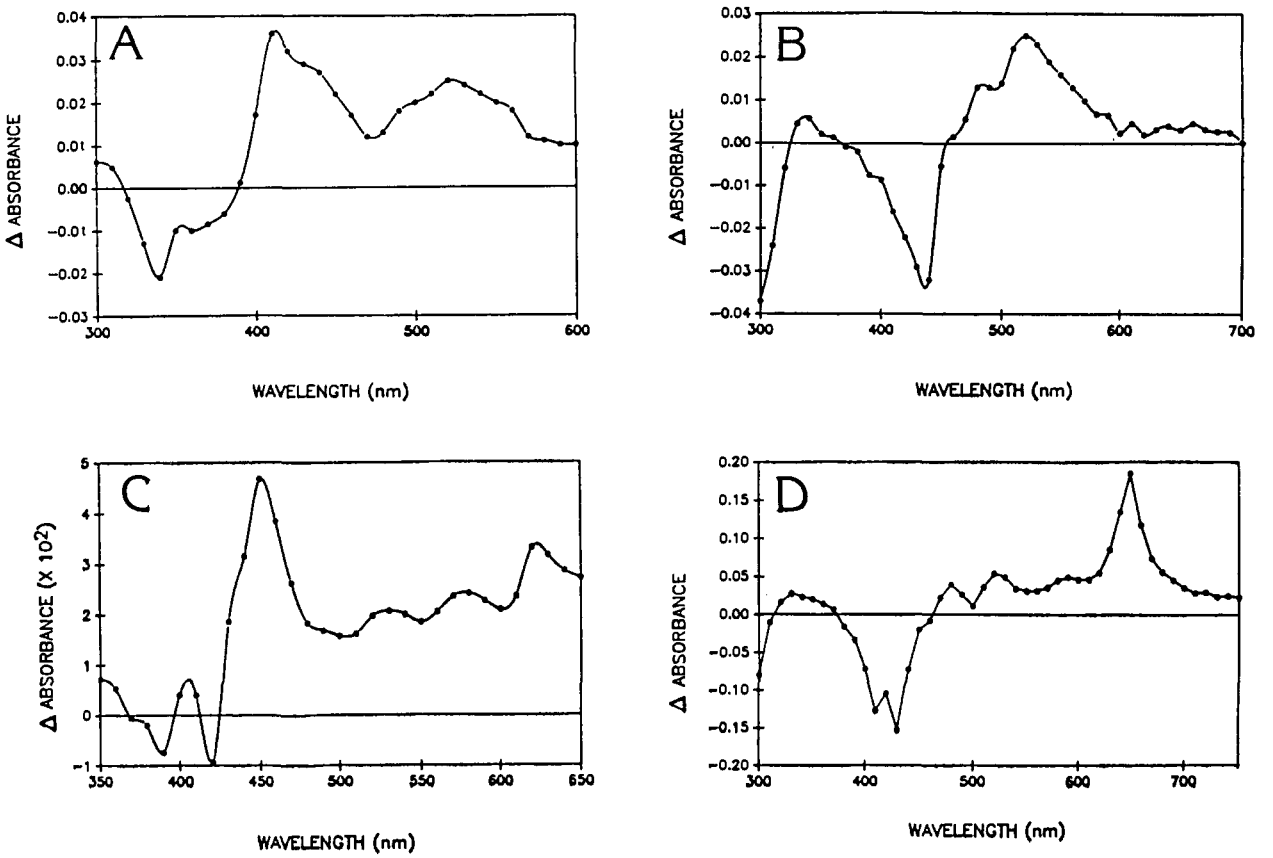

Figure 2. Triplet-excited-state differential absorption spectra recorded for (a) DAP^{2+} and (b) $ADIQ^{2+}$ after excitation in N_2-saturated, neutral aqueous solution with a 10-ns laser pulse at 355 nm. Differential absorption spectra recorded for (c) $DAP^{\bullet+}$ and (d) $ADIQ^{\bullet+}$ under pulse radiolytic conditions.

Table II. Association Constants, Free Energy Changes for Electron Abstraction from the Base, and Kinetic Parameters Derived for the Radical Ion Pairs

salt	base	K^a (M^{-1})	F_q (%)	$\tau_{com}{}^a$ (ns)	$\Delta G^{\circ\,b}$ (eV)	$\tau_{rip}{}^a$ (ns)	$F_{esc}{}^a$ (%)	k_{rec} (μs^{-1})	k_{esc} (μs^{-1})
DAP^{2+}	dAMP	97	69	3.2	−0.79	80	22	9.7	2.7
DAP^{2+}	dCMP	20	58	4.2	−0.56	140	33	4.7	2.3
DAP^{2+}	dGMP	170	74	2.8	−0.91	50	16	16.8	3.2
$ADIQ^{2+}$	dAMP	2300	47	14.0	−0.23	93	28	7.7	3.0
$ADIQ^{2+}$	dCMP	1100	−14[c]	27.0	0.02				
$ADIQ^{2+}$	dGMP	4300	79	5.3	−0.33	90	15	9.4	1.7

[a] ±10%. [b] Calculated according to ref 33; ±10 kJ mol^{-1}. [c] An enhancement of 14% is observed in this case.

with bimolecular rate constants of $(2.0 \pm 0.3) \times 10^9$ M^{-1} s^{-1}. Quantum yields for formation of singlet oxygen (Φ_Δ) are collected in Table I and are seen to reflect the quantum yields for population of the triplet state (Φ_t). These values are not high but indicate that the quaternary salts could function as triplet-state sensitizers in water.

Cyclic voltammetry studies carried out in N_2-saturated, neutral aqueous solution show that both DAP^{2+} and $ADIQ^{2+}$ undergo two single-electron reduction steps. Both processes are diffusion-controlled but poorly reversible due to adsorption of the reduction product onto the electrode surface. In organic solvents, such as acetonitrile or *N,N*-dimethylformamide, the reduction steps are reversible.[14,28] Peak potentials for the first ($E_p{}^1$) and second ($E_p{}^2$) reductions, as measured at slow scan rates (20 mV s^{-1}) in aqueous solution, are given in Table I. The potential differences between addition of the first and second electrons ($\Delta E = E_p{}^2 - E_p{}^1$) are −130 and −160 mV, respectively, for $ADIQ^{2+}$ and DAP^{2+}. These latter values can be used to calculate disproportionation constants for the one-electron-reduction products (K_{dis}), and the derived values (Table I) imply that the products should be susceptible toward disproportionation to the two-electron-reduced species at high concentrations.

Absorption spectra for the one-electron-reduction products were recorded by the pulse radiolytic technique following reduction by the hydrated electron and, for DAP^{2+}, the 2-hydroxypropyl radical. These products are assigned to the corresponding radical cations:

$$DAP^{2+} + e_{aq}{}^- \rightarrow DAP^{\bullet+} \quad (1)$$

$$DAP^{2+} + (CH_3)_2COH \rightarrow DAP^{\bullet+} + H^+ + (CH_3)_2CO \quad (2)$$

$$ADIQ^{2+} + e_{aq}{}^- \rightarrow ADIQ^{\bullet+} \quad (3)$$

The spectrum observed for $DAP^{\bullet+}$ (Figure 2c) agrees well with that obtained previously from steady-state photolysis of DAP^{2+} in the presence of sacrificial reducing agents[11] while the spectrum observed for $ADIQ^{\bullet+}$ is given in Figure 2d.

Interaction between Quaternary Salts and Nucleotides. Fluorescence from the quaternary salts was quenched by the individual nucleotides dAMP, dCMP, and dGMP in neutral aqueous solution containing 5 mM phosphate buffer (μ = 30 mM). Stern–Volmer plots constructed from fluorescence yields were markedly nonlinear whereas the corresponding plots constructed from fluorescence lifetimes were linear over a limited (0–15 mM) concentration range. Addition of the nucleotides caused adsorption

(28) For pyrene in dimethylformamide, half-wave potentials for addition of one and two electrons, respectively, are −2.41 and −2.88 V vs NHE (Given, P. H.; Peover, M. E. *J. Chem. Soc. B* **1960**, 385). Thus, the presence of two *N*-methylaza substituents brings about a substantial increase in both half-wave potentials and decreases the peak separation.

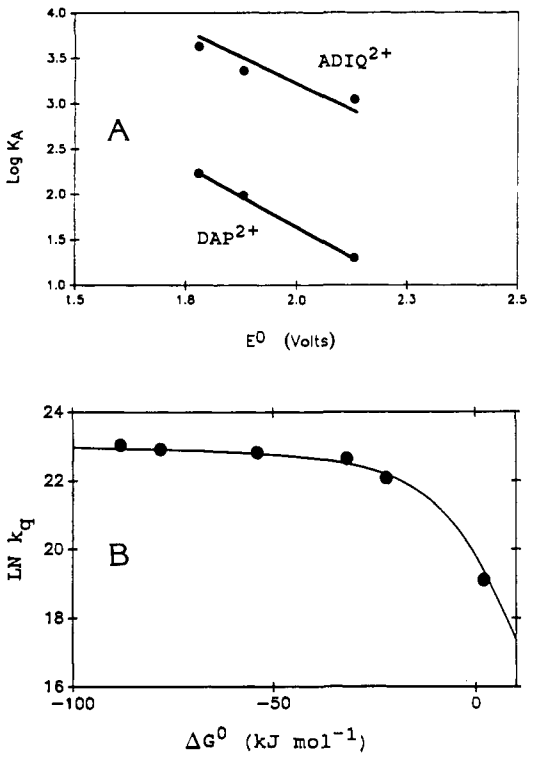

Figure 3. (a) Correlation between association constant and oxidation potential of the base for the two dyes. (b) Semilogarithm plot of the fluorescence quenching rate constant versus the thermodynamic driving force for electron abstraction from the nucleic acid base. The curve is a fit to the Rehm–Weller model[34] with a diffusional rate constant of 1.5×10^{10} M^{-1} s^{-1} and a free energy of activation change at $\Delta G^\circ = 0$ of 12 kJ mol^{-1}.

and fluorescence spectral shifts, spectra being broadened and red-shifted.[12,13] Such behavior indicates that both static and dynamic fluorescence quenching processes prevail.[29] Bimolecular quenching rate constants (k_q) were derived from the lifetime studies, over the linear range, whereas the absorption spectral changes were analyzed in terms of the Benesi–Hildebrand model[30] to obtain association constants (K) characteristic of the static quenching process. Both quaternary salts form mono- and bis-complexes with added nucleotide, but the relevant association constants are disparate and, for our studies, only monocomplexation was characterized.

Complexation is more pronounced for the more hydrophobic $ADIQ^{2+}$, and for both dyes, K depends on the nature of the base (Table II). Since each nucleotide carries identical phosphate and ribose functions, this latter finding may indicate that complexation involves mainly hydrophobic stacking between dye and base, as described for acridine derivatives.[31] Indeed, there is a clear correspondence between K and the redox potential for one-electron oxidation of the base[32] (Figure 3a) that is consistent with complexation involving partial charge-transfer interactions between stacked macrocycles. Our measured K values are consistent with literature values (for DAP^{2+}/adenine,[11] log K = 2; for $ADIQ^{2+}$/adenosine,[13] log K = 2.53; for $ADIQ^{2+}$/dAMP,[13] log K = 3.64), although the values are ionic strength dependent and increase with increasing number of phosphate groups.[13] These latter effects demonstrate that electrostatic binding is important in the overall complexation process.

Fluorescence quenching was accompanied by a corresponding decrease in formation of the triplet excited state of the quaternary

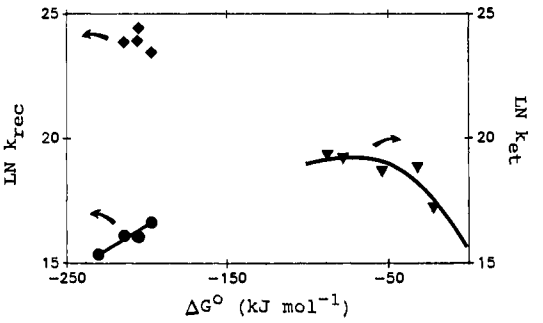

Figure 4. Correlations between reaction exothermicity and rate constants for forward (▼) and reverse (●) electron transfer within dye/nucleotide complexes and (◆) for reverse electron transfer for intercalated dye. The lines drawn through the data points are fits to (▼) eq 4 and (●) eq 5, as mentioned in the text.

Scheme I. Reaction Scheme Indicating Electron-Transfer Pathways for Both Separated and Complexed Dye/Nucleotide Systems

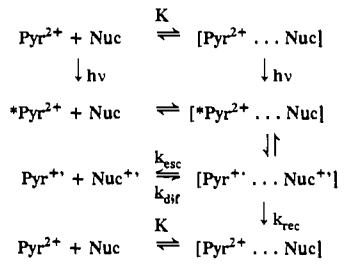

salt, although the triplet lifetime remained essentially unchanged, and in the formation of singlet molecular oxygen. Thus, quenching does not result in enhanced population of the triplet manifold, and instead, it is attributed to photoinduced electron abstraction from the base by the singlet excited state of the quaternary salt. There are modest thermodynamic driving forces for electron abstraction (ΔG°)[33] that correlate with the measured k_q values. Indeed, the observed bimolecular quenching behavior can be described in terms of the Rehm–Weller[34] empirical model for diffusional electron transfer with an activation free energy change at $\Delta G^\circ = 0$ of 12 kJ mol^{-1} and a diffusional limit of 1.5×10^{10} M^{-1} s^{-1} (Figure 3b). The high diffusional limit indicates that reaction is assisted by Coulombic attraction between the reactants.

Photophysical studies were performed for each of the dye/nucleotide ground-state complexes, under conditions where most (>95%) of the dye was present as a 1/1 complex. Fluorescence quantum yields and lifetimes were measured and compared to values determined in the absence of nucleotide (Table II). It is seen that the extent of fluorescence quenching upon complexation ($F_q = [1 - \Phi_f/\Phi_f^\circ]$) follows the values of ΔG° estimated for photoinduced electron transfer from base to dye. There is a similar decrease in fluorescence lifetime (τ_{com}), and as described below, redox products are observed after decay of the excited singlet state. As such, fluorescence quenching is assigned to net electron transfer in accordance with Scheme I.

With $ADIQ^{2+}$/nucleotide complexes, fluorescence decay profiles could be analyzed satisfactorily in terms of a single exponential component; note, with cytosine the observed lifetime for the complex exceeds that measured for free dye.[35] However, for DAP^{2+} the decay profiles contained minor components attributed to the biscomplexes.[36] With use of the lifetime data, rate constants

(29) Nemzek, T. L.; Ware, W. R. *J. Chem. Phys.* **1975**, *62*, 477.
(30) Benesi, H.; Hildebrand, J. *J. Am. Chem. Soc.* **1949**, *71*, 2703.
(31) Hosseini, M. W.; Blacker, A. J.; Lehn, J.-M. *J. Chem. Soc., Chem. Commun.* **1988**, 596.
(32) Redox potentials for one-electron oxidation of guanine, adenine, and cytosine (E_{ox}), respectively, are 1.78, 1.88, and 2.13 V vs NHE (Loeber, G.; Kittler, L. *Stud. Biophys.* **1978**, *73*, 25).
(33) Calculated according to $\Delta G^\circ = -F[E_p^1 - (E_{ox} - E_s)]$, where E_s refers to the electronic energy of the first excited singlet state of the quaternary salt, as measured from absorption and fluorescence spectroscopy. Incidently, it was observed that ribose did not quench the fluorescence of DAP^{2+} or $ADIQ^{2+}$, even at concentrations as high as 1 M.
(34) Rehm, D.; Weller, A. *Isr. J. Chem.* **1970**, *8*, 259.
(35) There is no obvious explanation for the increased lifetime observed for the $ADIQ^{2+}$/dCMP complex. It may indicate that $ADIQ^{2+}$ is partly associated with a chloride ion, which acts as an ineffective quencher. Ion pairing between the quaternary salt and the phosphate group may displace the chloride ion and give enhanced fluorescence.

for intracomplex electron transfer ($k_{et} = (1/\tau_{com}) - (1/\tau_s)$) were derived (for monocomplexes only) and are seen to depend on the thermodynamic driving force (Figure 4). Assuming each of the complexes possesses comparable geometric features, it should be expected that k_{et} correlates with the reaction exothermicity according to conventional theory:[37]

$$k_{et} = (2\pi/\hbar)|V(r)|^2\text{FCWD} \quad (4)$$

where $V(r)$ is the electron exchange matrix element and FCWD represents the Franck–Condon weighted density of states. Although the paucity of derived k_{et} values prevents meaningful analysis, the data can be fit to eq 4 with a limiting rate constant of ca. 5×10^8 s^{-1} and a total reorganization energy term of ca. 85 kJ mol^{-1}. This is an unexceptional reorganization energy,[37] but the limiting rate constant is some 200-fold lower than typically observed with contact charge-transfer complexes in organic solvents.[38] This latter effect most probably relates to the structure of the complexes and could be explained[37] in terms of a dye/base internuclear separation distance of ca. 10 Å.

Laser flash photolysis studies, using a 10-ns excitation pulse at 355 nm, were carried out for the various complexes. It was observed that the radical cation of the quaternary salt was present at the end of the pulse,[39] except for the ADIQ^{2+}/dCMP complex, which showed only triplet-state ADIQ^{2+}. The observed radical cations decayed via first-order kinetics to leave a residual transient that retained the same absorption spectrum but persisted over many microseconds. The fast process is ascribed to charge recombination within a radical ion pair while the longer lived transient is attributed to radical cation that escapes geminate recombination by way of dissociation of the radical ion pair (Scheme I). Decay of separated products occurs by way of diffusional recombination (k_{dif}). Lifetimes measured for the various radical ion pairs (τ_{rip}) and the fractions of radical cation that escape geminate recombination (F_{esc}) are collected in Table II.

The radical ion pairs survive for a surprisingly long time. Assuming that decay of the radical ion pair involves only geminate recombination (k_{rec}) or escape from the cage (k_{esc}), the individual rate constants can be resolved (Table II). Although restricted to a few data points, it appears that k_{esc} can be approximated[40] to a constant value of $\sim 3 \times 10^6$ s^{-1}, which is very slow (cf. k_{esc} values of ca. 5×10^9 s^{-1} usually encountered for weakly bound radical ion pairs in organic solvents[41]). We interpret this behavior in terms of the radical ion pairs being held together by strong hydrophobic forces, together with electrostatic interactions, such that the rate of separation is kept to a minimum.

The rate of geminate recombination shows a weak dependence on the thermodynamic driving force (Figure 4). Extremely large amounts of energy have to be dissipated during this process such that it is expected to lie well within the Marcus inverted region.[42] Mataga and co-workers[43] have argued that k_{rec} for contact ion pairs can be expressed in terms of eq 5, where α and β are constants independent of $\Delta G°$. This equation, which has been used successfully to describe the dynamics of a variety of radical ion pairs[44] and which is analogous to that used to express the radiationless transition probability in the weak coupling limit,[45] accounts for our data with $\alpha = 1.8 \times 10^{10}$ s^{-1} and $\beta = 3.4$ eV^{-1} (Figure 4). Our derived β is consistent with the shallow dependence of k_{rec} on $\Delta G°$ observed by Mataga and co-workers[43] in their systems, but our extrapolated value of α is extremely low. As noted for the forward process, this may arise from structural features, such as a large internuclear separation distance or unfavorable orientation.

$$k_{rec} = \alpha \exp(-\beta[\Delta G°]) \quad (5)$$

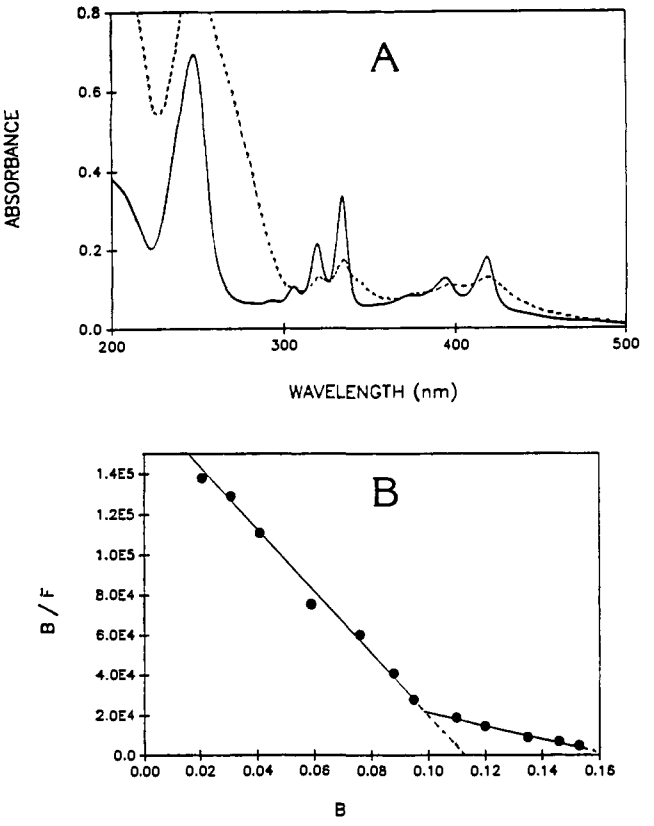

Figure 5. (a) Absorption spectra recorded for DAP^{2+} in neutral aqueous solution with and without excess DNA added (P/D = 30). (b) Scatchard plot for titration of DAP^{2+} with DNA. Data taken from fluorescence spectral measurements, with B being the molar ratio of complexed dye to DNA and F being the molar concentration of free dye. The association constant K is obtained from the slope, and the saturation number n is derived from the extrapolated intercept.

Table III. Association Constants (K) and Saturation Numbers (n), Expressed in Terms of Molecules of Dye per Base, Measured for the Quaternary Salts with Calf Thymus DNA in 5 mM Phosphate Buffer at pH 7

dye	K_1,[a] (M^{-1})	n_1[b]	K_2,[c] (M^{-1})	n_2[c]	K_3,[c] (M^{-1})	n_3[c]
DAP^{2+}	1.4×10^7	0.11	2.0×10^6	0.16		
ADIQ^{2+}	$>5 \times 10^8$		1.5×10^8	0.42	2.7×10^7	0.65

[a] ±10%. [b] ±0.05. [c] ±20%.

Binding to DNA. In accordance with earlier studies,[11-13] it was observed that both quaternary salts interacted strongly with calf thymus DNA in neutral aqueous solution. Interaction is characterized by a pronounced red shift, broadening and decrease in intensity of the dye absorption bands (Figure 5a), and a dramatic reduction in the fluorescence quantum yield. Analyzing the fluorescence titration data according to the Scatchard model[46-48]

(36) For the DAP^{2+}/nucleotide complexes, the fluorescence decay profiles contained minor contributions from shorter (ca. 1 ns) lifetimes, the percentage of which increased with increasing nucleotide concentration. These components are attributed to biscomplexes.

(37) Miller, J. R.; Beitz, J. V.; Huddleston, R. K. *J. Am. Chem. Soc.* **1984**, *106*, 5057.

(38) (a) Hirata, Y.; Saito, T.; Mataga, N. *J. Phys. Chem.* **1987**, *91*, 3119. (b) Ojima, S.; Miyasaka, H.; Mataga, N. *J. Phys. Chem.* **1990**, *94*, 4147, 5834, 7539.

(39) The resultant oxidation products derived from the nucleic acid bases are expected to exhibit featureless and weak absorption spectra in the visible region that contain no characteristic bands. See: Jovanovic, S. V.; Simic, M. G. *J. Phys. Chem.* **1986**, *90*, 974.

(40) It is common policy to consider k_{esc} as a constant for a given set of contact ion pairs and, thereby, regard differences in yields of separated products as arising from variations in k_{rec}. See: Gould, I. R.; Roger, M.; Farid, S. *J. Am. Chem. Soc.* **1988**, *110*, 7242.

(41) Spears, K. G.; Gray, T. H.; Huang, D. *J. Phys. Chem.* **1986**, *90*, 779.

(42) Marcus, R. A. *J. Chem. Phys.* **1956**, *24*, 5057.

(43) (a) Asahi, T.; Mataga, N. *J. Phys. Chem.* **1989**, *93*, 6575. (b) Mataga, N. In *Perspectives in Photosynthesis*; Jortner, J., Pullman, B., Eds.; Kluwer Academic Publishers: Amsterdam, 1990; p 227.

(44) Asahi, T.; Mataga, N.; Takahasti, Y.; Miyashi, T. *Chem. Phys. Lett.* **1990**, *171*, 309.

(45) Englman, R.; Jortner, J. *Mol. Phys.* **1970**, *18*, 145.

(46) Scatchard, G. *Ann. N. Y. Acad. Sci.* **1949**, *51*, 660.

Table IV. Photophysical Properties Measured for the Quaternary Salts Intercalated into Polynucleotides (P/D = 30) in Neutral Aqueous Solution[a]

polymer	Φ_f/Φ_f^0	τ/τ^0	τ_1[b] (ns)	τ_2[c] (ns)	τ_3[c] (ns)	τ_{rec}[d] (ps)
			DAP^{2+}			
CT-DNA	0.017	0.43	0.4 (42)	2.7 (25)	9.3 (33)	45
poly[dG-dC]	0.055	0.29	0.3 (48)	2.8 (32)	7.7 (20)	68
poly[dA-dT]	0.160	0.93	2.1 (21)	10.0 (79)		41
			$ADIQ^{2+}$			
CT-DNA	0.046	0.26	2.2 (67)[e]	14.5 (33)[e]		
poly[dG-dC]	0.074	0.24	3.0 (71)	13.0 (29)		25
poly[dA-dT]	0.78	0.77	4.5 (53)	27.0 (47)		40

[a] The values given in parentheses after the lifetimes are the corresponding fractional amplitudes. [b] ±0.1 ns. [c] ±0.5 ns (±2%). [d] ±5 ps. [e] P/D = 7.

indicates that there are at least two resolvable binding modes (Figure 5b).[11-13] At high polynucleotide to dye (P/D) ratios, the dye appears to intercalate between base pairs; the intercalation constant (K_1) and base-pair saturation number (n_1) for DAP^{2+} are collected in Table III, but meaningful numbers could not be derived for $ADIQ^{2+}$.[13] At lower P/D ratios, secondary complexation is observed and association constants (K_2) and saturation numbers (n_2) are collected in Table III; for $ADIQ^{2+}$, the first (intercalation) and second binding processes appear to be highly cooperative and not decoupled.[13] For $ADIQ^{2+}$, a third binding process could be characterized and the derived K_3 and n_3 values are given in Table III. With use of synthetic polynucleotides, it was found that both dyes bind much more effectively to poly[dG-dC] than to poly[dA-dT]. Even for these synthetic polynucleotides, binding of dye molecules involves multiple steps.[13] As a tentative explanation of these results, we believe that dye molecules selectively intercalate between base pairs at high P/D (>20) ratios and, in addition, bind to the outer surface of the biopolymer at lower P/D (<5) ratios. Intercalation of such large polycycles must cause some distortion of the biopolymer, possibly providing an opening for a second dye molecule nearby. At very low P/D ratios, part of the dye appears to be present in an aggregated state. Our subsequent time-resolved studies were made at sufficiently high P/D (>20) ratios for intercalated dye molecules to predominate, although it has proved impossible to use conditions where only one binding site is occupied.

Pulse radiolysis studies were made with intercalated quaternary salt under reducing conditions. It was observed that hydrated electrons reduced the salts to the corresponding radical cation, in accordance with eqs 1-3, although the rate of reduction was relatively slow. This may arise from a Coulombic repulsive effect since the hydrated electron has to penetrate the phosphate shield. In deoxygenated solution, intercalated radical cation was stable and was not ejected from the DNA strand despite the decreased electrostatic binding energy. In fact, the negligible peak potential shifts observed in the cyclic voltammograms indicated[49] that the binding constants for salt and radical cation are similar.

Photochemistry of Intercalated Quaternary Salts. Intercalation of the quaternary salts is accompanied by reductions in the fluorescence quantum yield. The magnitude of the change (Φ_f/Φ_f^0), corrected for absorption spectral variations, shows a marked dependence on the nature of the polynucleotide for a P/D ratio of ca. 30 (Table IV) and increases according to poly[dA-dT] < poly[dG-dC] < DNA. Quenching depends also on the nature and concentration of the dye and on the P/D ratio.[13] Time-resolved fluorescence decay profiles required analysis in terms of multiexponential fits, with the relative fractions depending on dye concentration and P/D ratio. These findings indicate complex binding behavior, with dye molecules occupying several sites on the biopolymer and/or remaining free in solution. Experimental data collected at low dye concentration (<5 μM) and at P/D = 30 are compiled in Table IV.

Analytical fits to the time-resolved fluorescence profiles involved two or three exponentials (Table IV), but even so, integration of the decay curves (τ/τ^0) gives apparent fluorescence yields that are much too high when compared to the steady-state fluorescence data (Φ_f/Φ_f^0) (Table IV). This finding indicates that, with the possible exception of $ADIQ^{2+}$ binding to poly[dA-dT],[50] a substantial fraction of the excited singlet state decays on a time scale too short for us to observe.[51] Indeed, to satisfactorily account for all the fluorescence data, it is necessary that the major component decays with a lifetime $\tau < 20$ ps. On the basis of picosecond flash photolysis studies (see later text), this component is assigned to dye molecules that rapidly abstract an electron from an adjacent guanine or adenine base upon excitation. Rapid electron transfer should be expected[15] for intercalated DAP^{2+} and $ADIQ^{2+}$ since the internuclear separation distances will be only a few angstroms. From eq 4, and by using the experimental results obtained for dye/nucleotide complexes, k_{et} for intercalated material is expected to exceed 10^{11} s^{-1}; for methylene blue[15] intercalated into DNA, $k_{et} = 10^{12}$ s^{-1} and $\Delta G^\circ = -11$ kJ mol^{-1} for electron abstraction from guanine.

This being the case, the observed fluorescence decay profiles must correspond to dye molecules less favorably positioned with respect to rapid electron abstraction from a nucleic acid base. This may include dye molecules free in solution, loosely bound to the polymer surface, or incompletely intercalated. Electronic energy transfer may occur between some of these species,[52] further complicating the situation. With such a multitude of species present, it seems inappropriate to analyze the fluorescence decay profiles as the sum of exponential terms. Certainly, the data fit satisfactorily to a stretched exponential decay law.[53] The main point, however, is that a substantial fraction of intercalated dye undergoes rapid ($k > 5 \times 10^{10}$ s^{-1}) deactivation upon excitation in each biopolymer.[54]

Laser flash photolysis studies were conducted with the various polynucleotides at P/D ratios of 30. Much higher concentrations of dye are required for these studies, especially $ADIQ^{2+}$, which absorbs poorly at 355 nm, such that dye molecules are expected to be distributed among the available sites. Under these conditions, the $ADIQ^{2+}$/DNA system precipitated during the flash photolysis studies. Lower dye concentrations gave unreliable kinetic traces due to the poor signal-to-noise ratios whereas at lower concentrations of DNA high levels of background fluorescence, presumably from uncomplexed dye, obscured the absorption spectral information. Consequently, this system could not be studied under comparable conditions.

Following laser excitation with a 30-ps pulse at 355 nm, the characteristic absorption spectrum of the quaternary salt radical cation could be observed (Figure 6a,b). This species decayed rapidly via first-order kinetics to leave a pronounced background signal that decayed slowly (Figure 6c). The fast process is attributed to reverse electron transfer between the primary products for which the measured lifetimes (τ_{rec}) are collected in Table IV. In each case, $\tau_{rec} < 100$ ps and the products must arise from the

(47) Klotz, I. M. *Science* **1982**, *217*, 1247.
(48) Davila, J.; Harriman, A. *J. Am. Chem. Soc.* **1990**, *112*, 2686.
(49) Carter, M. T.; Rodriguez, M.; Bard, A. J. *J. Am. Chem. Soc.* **1989**, *111*, 8901.

(50) For the $ADIQ^{2+}$/poly[dA-dT] system, τ_2 exceeds the fluorescence lifetime measured in the absence of biopolymer and this leads to an anomalously high τ/τ_0 value. When due allowance is made for this long τ_2, it becomes clear that there must be an additional short-lived component that cannot be resolved with our instrumental response (fwhm = 50 ps).
(51) In most of the fluorescence decay records, an instrument-broadened fast component was observed but, after deconvolution, its lifetime could only be determined to be <20 ps.
(52) Mergny, J.-L.; Slama-Schwok, A.; Montenay-Garestier, T.; Rougée, M.; Hélène, C. *Photochem. Photobiol.* **1991**, *53*, 555.
(53) (a) Siebrand, W.; Wildman, T. A. *Acc. Chem. Res.* **1986**, *19*, 238. (b) Hirayama, S.; Sakai, Y.; Ghiggino, K. P.; Smith, T. A. *J. Photochem. Photobiol., A* **1990**, *52*, 27.
(54) We observed overall fluorescence quenching for $ADIQ^{2+}$ bound to poly[dA-dT], but ref 52 reports a 15% enhancement in fluorescence yield. To explain this discrepancy, we suggest that the fluorescence yield measured[52] in the absence of poly[dA-dT] ($\Phi_f = 0.53$) is lower than the "actual" value ($\Phi_f = 0.79$) due to concentration quenching. In fact, a common Φ_f for $ADIQ^{2+}$ bound to poly[dA-dT] can be calculated from the two sets of data ($0.79 \times 0.77 = 0.61$; $0.53 \times 1.15 = 0.61$).

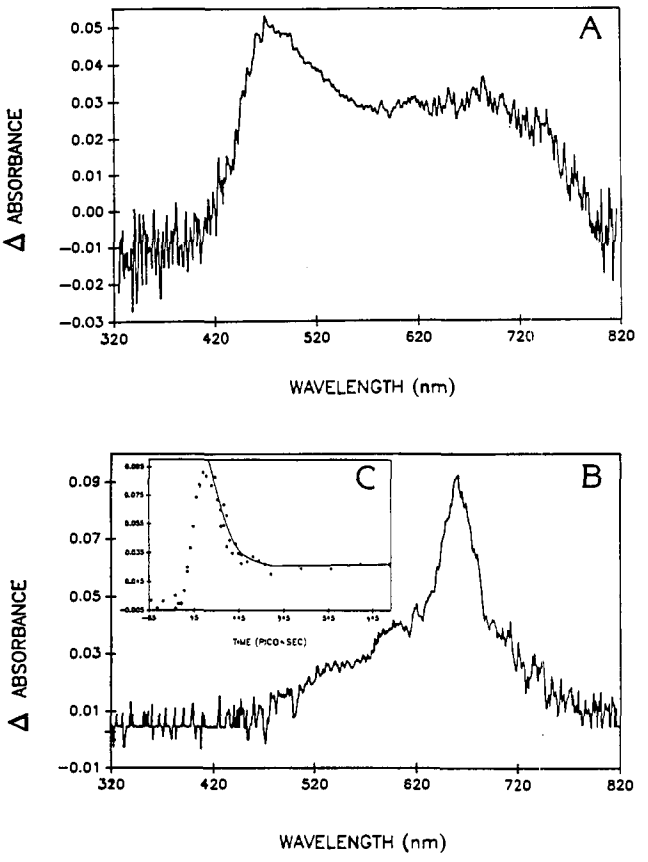

Figure 6. Transient differential absorption spectra recorded 30 ps after excitation of (a) DAP^{2+} and (b) $ADIQ^{2+}$ intercalated into poly[dG-dC] (P/D = 30). (c) Typical kinetic trace measured at 660 nm for system b above.

inferred rapid (i.e., < 20 ps) quenching of the dye excited singlet state. These rapid forward and reverse electron-transfer processes are believed to involve intercalated dye molecules and adjacent (guanine or adenine) bases. The longer lived transient absorbance corresponds to a mixture of the excited singlet state of dye molecules not able to undergo rapid electron abstraction from an adjacent base and, in some cases,[55] redox products formed on slower time scales. The long-lived excited singlet states give rise to the observed multiexponential fluorescence decay profiles and correspond to nonintercalated dye molecules. Data analysis was complicated by the multitude of overlapping transients and by our limited time window of 30 ps to 5 ns. No transient species survive for longer than about 30 ns.

The derived τ_{rec} values show no obvious dependence on the nature of the polynucleotide. With use of thermodynamic arguments, it seems reasonable to suppose that excited-state dye abstracts an electron preferentially from either guanine or adenine. The redox potentials for these two bases, as measured for isolated molecules in water,[32] differ by only 100 mV, which is insufficient to observe a correlation between the rate constant for reverse electron transfer ($k_{rec} = (\tau_{rec})^{-1}$) and the reaction exothermicity (Figure 4). A value for τ_{rec} of 130 ps reported[15] for DNA-intercalated methylene blue, where $\Delta G°$ is −177 kJ mol^{-1}, is comparable with our data and consistent with reverse electron transfer occurring within the inverted region.[42] Comparison of the derived k_{el} and k_{rec} values for intercalated dye and for dye complexed to nucleotides (Figure 4) shows that the former rates are about 2500 times faster. This is entirely consistent with the smaller internuclear separations that should arise from intercalation.

Conclusion

The singlet excited states of DAP^{2+} and $ADIQ^{2+}$ undergo reversible electron-transfer reactions with nucleic acid bases in fluid solution, within complexes, and after intercalation into polynucleotides. The time scales for both forward and reverse steps depend on the identity of the base and, more importantly, on the structure of the precursor complex. Because of the large amount of energy to be dissipated, reverse electron transfer falls well within the inverted region[42] and, for a given reactant pair, is always slower than the forward reaction. The rate of reaction is believed to decrease with increasing internuclear separation distance, as modulated by the nature of the complex. These findings are in keeping with nonadiabatic electron-transfer theory.[37]

Time-resolved fluorescence studies indicate that association between the dyes and polynucleotides is complex and involves location of the dye at a variety of sites.[13] The relevant binding constants are not disparate, and binding could be cooperative. Under illumination, intercalated dye molecules abstract an electron from an adjacent guanine or adenine but the reaction is highly reversible. Such processes cannot, therefore, be responsible for the photochemical strand scission known to occur with these dyes.[12b] In contrast, dye molecules free in solution or loosely bound to the phosphate layer do not undergo photoinduced electron-transfer reactions with the bases. Free dye molecules, by virtue of photoreduction by ribose (ultimately forming hydrogen peroxide) or production of $O_2(^1\Delta_g)$, are able to realize strand scission.

Acknowledgment. This work was supported by the Texas Advanced Research Program. We thank Dr. S. J. Atherton, Dr. S. M. Hubig, B. K. Naumann, and P. T. Snowden for technical assistance and Professor Jean-Marie Lehn for helpful discussions. The CFKR is supported jointly by the Biomedical Research Technology Program of the Division of Research Resources of the NIH (Grant RR00886) and by the University of Texas at Austin.

Registry No. DAP^{2+}, 21178-14-3; $ADIQ^{2+}$, 118891-86-4; dAMP sodium salt, 50611-39-7; dCMP sodium salt, 75652-48-1; dGMP sodium salt, 87713-30-2; poly[dA-dT] sodium salt, 86828-69-5; poly[dG-dC] sodium salt, 90385-88-9.

(55) In these experiments, it is difficult to completely compensate for fluorescence originating from nonintercalated dye and this problem restricts the usable spectral range. After the initial recombination, the residual species is the excited singlet state of the dye. There is no spectroscopic evidence to indicate a second (slower) crop of reduced dye, suggesting that, for nonintercalated dye molecules that undergo electron-transfer quenching, the rate of the reverse step exceeds that of the forward process.